Applied Surface Science 258 (2012) 4199–4202

Contents lists available at ScienceDirect

Applied Surface Science

journal homepage: www.elsevier.com/locate/apsusc

Properties of nanopatterned pins generated in a superconductor with FIB

Gorky Shaw [a], Pabitra Mandal [a], Biplab Bag [a], S.S. Banerjee [a,*], T. Tamegai [b], Hermann Suderow [c]

[a] Department of Physics, Indian Institute of Technology, Kanpur 208016, U.P., India
[b] Department of Applied Physics, The University of Tokyo, Hongo, Bunkyo-ku, Tokyo 113-8656, Japan
[c] Laboratorio de Bajas Temperaturas, Departamento de Fiїsica de la Materia Condensada Instituto de Ciencia de Materiales Nicolaїs Cabrera, Facultad de Ciencias Universidad Autonoma de Madrid, E-28049 Madrid, Spain

ARTICLE INFO

Article history:
Available online 10 May 2011

Keywords:
Nanoscale
Patterning
Focused ion beam
Superconductivity
Vortex state
Pinning

ABSTRACT

We have used focused ion-beam to nanopattern an array of artificial pinning centers on the surface of a superconductor. By investigation of the bulk as well as local magnetization responses we find that the pinning properties of the artificially generated pins differ significantly from those in an unpatterned superconductor with natural pinning centers. The gradients in the magnetic field distribution inside the nanopatterned region have very different field dependences compared to those outside it. The non-equilibrated nature of the flux distribution due to artificial pins is associated with a magnetization response which is dependent on the rate at which magnetic field is swept during the measurements. The array of artificially generated pins produces large increases in pinning force at large drives and at high fields, which potentially could help in enhancing the current carrying capability of superconductors especially at high fields.

1. Introduction

Enhancing the amount of current which can be carried by a superconductor placed in a magnetic field without producing dissipation (viz., enhancement of the critical current density, J_c) and also to reliably control the J_c is of technological importance for energy efficient devices. Usually the J_c of a superconductor decreases with increasing magnetic field. In the mixed phase of type II superconductors placed in a magnetic field the superconducting medium separates into microscopic normal and superconducting regions. String like entities called vortices, which have a normal core and carry a single flux quantum, enter the sample, thread throughout the whole thickness of the sample. When applying a current, vortices are subject to the Lorentz force, and, above a threshold current, called Jc, they start drifting and produce dissipation. To prevent dissipation and hence enhance Jc requires immobilizing the vortices, which needs generating vortex pinning centers in the material, at length scales which are in many materials of the order of a few nanometers. Controlled generation of pinning centers in recent times has been made possible by nanoscale engineering of pinning centers. Such nanoengineered pinning sites are considered very effective for trapping and immobilizing vortices which in turn enhance the J_c of the superconductor [1–4]. Typical dimensions of the pinning centers are comparable to the length scales which characterize vortices, namely the coherence length (ξ, approximately giving the size of the core) or the penetration depth (λ, approximately giving the shape of the magnetic field profile around the core). While previous studies have generally focused on creating superconductors with homogeneous artificial pinning centers [1–4], here, we have investigated samples in which we created a mixture of pinning centers. Using the focused ion beam (FIB), we have nanopatterned a small area of a superconductor with a regular array of holes. The artificially engineered pinning centers coexist with random distribution of point pins which are naturally present in the sample. Since the nanopatterned area does not cover the entire sample surface therefore the pinning due to the artificial pins does not overwhelm pinning properties in the sample. This allows us to compare the pinning properties generated with the artificial pins vis-à-vis the naturally occurring pins in the sample. Also by patterning the holes on a single crystal sample of a superconductor we have departed from most of the earlier studies where artificial pins were generated on superconducting films [5]. We observe a significant enhancement in pinning response of the nanopatterned sample which is drive dependent. The increase in pinning is not related to changes in the equilibrium properties of the vortex state in superconductors [1,6,7]. By locally imaging the distribution of magnetic fields around the nanopatterned region of the sample with magneto-optical imaging we observe the patterned array sustains large gradients in magnetic field distribution which are absent in the unpatterned regions of the sample. These magnetic field gradients around the patterned region are affected in different ways for a field step applied at low and at comparatively higher fields. The array of artificially generated pins leads to a highly non-equilibrium configuration of field distribution inside the sam-

* Corresponding author. Tel.: +91 512 2597559.
E-mail address: satyajit@iitk.ac.in (S.S. Banerjee).

0169-4332/$ – see front matter © 2011 Elsevier B.V. All rights reserved.
doi:10.1016/j.apsusc.2011.05.011

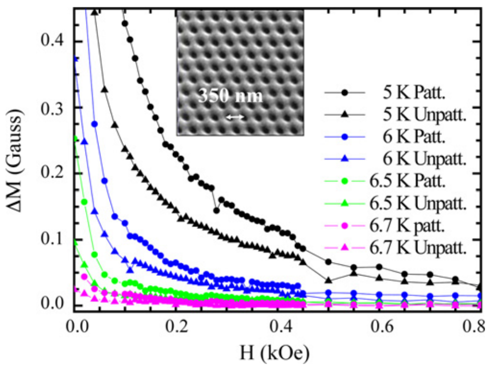

Fig. 1. Width of the magnetization hysteresis loop (ΔM) as a function of H obtained from isothermal bulk dc magnetization hysteresis $M(H)$ loops of the patterned and unpatterned $NbSe_2$ samples (denoted by circles and triangles respectively) measured at different temperatures using SQUID magnetometer. Inset shows an SEM image of a region of the 2H–$NbSe_2$ crystal patterned with the hexagonal array of blind holes.

ple as compared to naturally occurring pins. The drive dependent enhancement in J_c at high fields is achieved by partially nanoengineering a single crystal superconductor which could provide an unusual way to enhance the pinning force and hence the current carrying capability of superconductors especially at high fields.

2. Experimental details, results and discussion

2.1. Sample preparation

Our measurements are reported on two single crystals of 2H–$NbSe_2$ (the two crystals are cleaved from one single sample) belonging to a batch [7] of high quality single crystals (with similar dimensions ~1.5 mm × 1 mm × 30 μm, and $T_c(0) = 7$ K). One of the crystals was milled with a focused Ga ion beam (diameter ~ 7 nm) using the Focused Ion Beam (FIB) machine (dual beam FEI make Nova 600 NanoLab) to produce a hexagonal array of blind holes covering a rectangular area of ~180 μm^2 in the sample. An image of the patterned region is shown in the inset of Fig. 1. Each hole has a diameter of 170 nm (which is of the order of the superconducting penetration depth $\lambda_{ab} \sim 120$ nm for the 'ab' crystal orientation in 2H–$NbSe_2$) and a mean center-to-center spacing between the holes (d) of 350 nm and depth of ~1 μm. Bulk magnetization (M) response was measured using a Quantum Design Superconducting Quantum Interference Device (SQUID) magnetometer and a Vibrating Sample magnetometer (VSM). We also patterned a $Bi_2Sr_2CaCu_2O_8$ (BSCCO, $T_c \sim 90$ K) single crystal with blind holes identical to 2H–$NbSe_2$ for magneto-optical imaging studies. The total milling area in BSCCO viz., 44 μm × 39 μm, was chosen to be larger than that of 2H–$NbSe_2$ for convenience in performing optical imaging experiments (our setup details are mentioned in Ref. [8]).

2.2. Comparison of the magnetization response in patterned and unpatterned samples of 2H–$NbSe_2$

The width of the magnetization hysteresis loop viz., $\Delta M(H) = M_{\mathrm{forward}}(H) - M_{\mathrm{reverse}}(H) \propto J_c(H)$, is a measure of the pinning in the superconductor [9]. Fig. 1 main panel compares the widths $\Delta M(H)$ of the hysteresis loops for the patterned and unpatterned samples. It appears that nanopatterning with blind holes leads to enhanced widths at smaller fields (<0.3 kOe), however at higher fields the $\Delta M(H)$ for the two samples closely match. While the data in Fig. 1 was recorded with the magnetic field being stabilized at every field value, one may record the $M(H)$ loop when the magnetic field is swept.

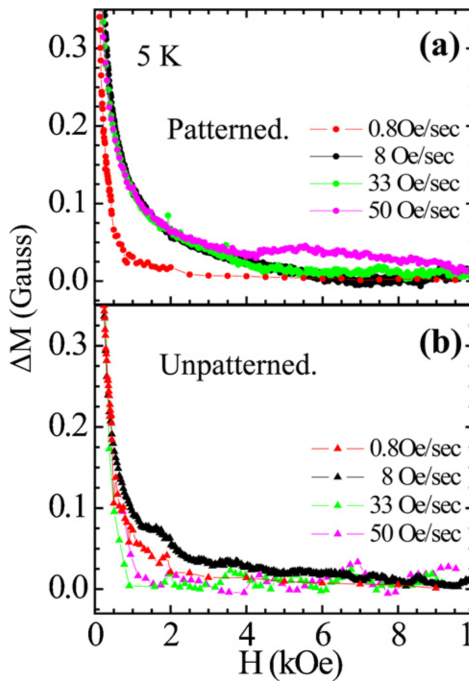

Fig. 2. $\Delta M(H)$ at 5 K for the (a) patterned and (b) unpatterned 2H–$NbSe_2$ samples for different field sweep rates $\beta \sim 0.8$, 8, 33 and 50 Oe/s.

In Fig. 2 we determine ΔM plots from measurements of the $M(H)$ hysteresis loops recorded when the magnetic field is swept at different rates ($\beta = dH/dt$) in a VSM. Fig. 2 reveals significantly drive dependent magnetization response at high fields. While in Fig. 1 we had found that the difference between the widths of the hysteresis loop for the patterned and unpatterned samples diminished at high fields in equilibrated field measurements, in swept field measurements significant difference appears. At low fields less than 0.5 kOe, in the unpatterned sample (Fig. 2(b)) there is almost no β dependence, while in the patterned sample, (Fig. 2(a)) in the same field regime, the width ΔM increases significantly with β. At fields above 0.5 kOe in the unpatterned sample (Fig. 2(b)) one finds that the ΔM decreases with β, while in the patterned sample the situation is exactly opposite. It appears that in the unpatterned sample due to larger screening currents induced at higher β, the irreversible magnetization response of the superconductor quickly tries to approach closer to the equilibrium magnetization behavior which leads to a lower ΔM with increasing β. In contrast, in the patterned sample it appears that with increase in β, say from 0.8 Oe/s to 8 Oe/s (Fig. 2(b)), the magnetization response becomes more irreversible, with the ΔM increasing with β. However for $\beta > 8$ Oe/s (Fig. 2(b)) we do not find a significant change in ΔM till a field of 3 kOe. In the field range of 3–10 kOe the $\Delta M(H)$ behavior in the patterned sample becomes nonmonotonic (close to 4 kOe, Fig. 2(b)) with a significant increase in ΔM with increasing β. In the same field range there is almost no field dependence of ΔM on β for the unpatterned sample.

2.3. Increase in pinning force at high fields and field sweep rate dependence

Fig. 3(b) compares pinning force curves at $T = 5$ K (using, $F_p(H) \propto \Delta M \times H$; as $J \propto \Delta M$) for the unpatterned sample (recorded at 50 Oe/s, black dashed curve) and the patterned sample (at different sweep rates as indicated, colored curves). Below 3 kOe, the weak pinning nature at low β in the patterned sample is evident from the coincidence of its $F_p(H)$ curves with that for the unpatterned sample at 50 Oe/s. In this field range, the $F_p(H)$ displays a peak like